# Fusion Imaging of Computed Tomography and 3D Echocardiography: Combined Assessment of Coronary Anatomy and Myocardial Function

Francesco Maffessanti, Karima Addetia, Gillian Murtagh, Lynn Weinert, Amit R Patel, Roberto M Lang, Victor Mor-Avi

University of Chicago, Chicago, IL, USA

## Abstract

*Cardiac multimodality imaging offers new opportunities to display composite information not available with any of the imaging modalities alone. We tested the feasibility of fusion of coronary anatomy and left ventricular (LV) function obtained from computed tomography coronary angiography (CTCA) and 3D echocardiography (3DE). Twenty-four patients underwent CTCA and transthoracic 3DE imaging on the same day. CTCA images were processed using custom software to extract the coronary tree. LV endocardial surfaces were obtained from 3DE and co-registered with the coronary tree using a rigid transformation. Three patients (12%) were excluded because of suboptimal CTCA quality. The composite display of coronary arteries and parametric images of regional LV function allowed visual appreciation of the LV functional abnormality secondary to the stenosis when present. Fusion of CT coronary angiography and parametric imaging of LV regional function derived from 3DE is feasible, potentially providing physiologically meaningful and easy-to-interpret combined display of coronary abnormalities and their functional impact.*

## 1. Introduction

Computed tomography coronary angiography (CTCA) is increasingly used as an alternative to invasive diagnostic coronary angiography [1,2], and is gaining wide clinical acceptance for its ability to rule out significant stenosis with high negative predictive value [3]. However, CTCA tends to overestimate the severity of stenosis and, from the perspective of revascularization, the extent of myocardial ischemia is more important than the degree of stenosis.

Recent studies have demonstrated that analysis of echocardiographic images using speckle-tracking techniques allows fast quantitative measurements of different components (longitudinal, radial and circumferential) of myocardial strain and function [4]. These techniques, initially applied to 2D images, were more recently shown to provide even more accurate information when applied to 3D images [5], eliminating the problem of out-of-plane motion.

One of the most recent developments in cardiac imaging is "fusion" of different modalities, which involves spatial registration and rendering of different aspects of cardiac anatomy and physiology in a single display. Fusion imaging allows reconciling individual findings obtained using different imaging modalities, with improved ease and confidence of diagnosis.

Our hypothesis was that 3DE measurements of myocardial strain could be integrated with the CTCA-derived 3D display of the coronary arteries, to aid in the evaluation of the functional effects of coronary stenosis, without the need for stress testing. Therefore our goal was to test the feasibility of this approach.

## 2. Methods

We enrolled 24 consecutive patients who underwent clinically indicated CTCA and agreed to perform transthoracic 3DE imaging on the same day. Figure 1 shows the workflow of the current study.

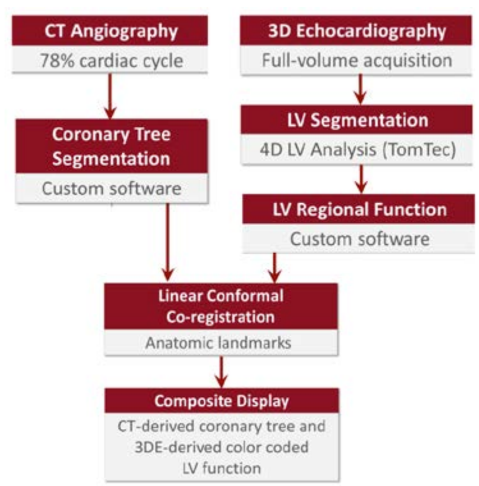


Figure 1. Schematic of the workflow from image acquisition to image fusion.

## 2.1. 3DE image acquisition

Transthoracic 3DE dataset were acquired using the iE33 ultrasound imaging system (Philips) equipped with a matrix array transducer (X5) in the full-volume mode. Imaging was performed using ECG gating during a single breath-hold.

## 2.2. CT image acquisition

CTCA was performed according to standard clinical protocol. Images were acquired (256-channel iCT scanner, Philips) during suspended respiration using retrospective gating in diastasis. Imaging parameters were: 270 ms gantry rotation time, slice thickness 0.625 mm, tube currents 600-1000 mA and voltage 100-120kV (depending on body weight). An iodinated contrast agent (approximately 65 ml, 5 ml/s) was infused, followed by a 20 ml bolus of normal saline.

## 2.3. Image analysis

3DE datasets were first analyzed using commercial software (4D LV-Analysis, TomTec Imaging Systems) designed to track ultrasound speckles in the myocardium in 3D space and measure longitudinal ($L_S$), radial ($R_S$) and circumferential ($C_S$) components of regional myocardial strain. Strain is defined as the percent ratio of total deformation to the initial dimension in the specific direction, as shown in Figure 2.

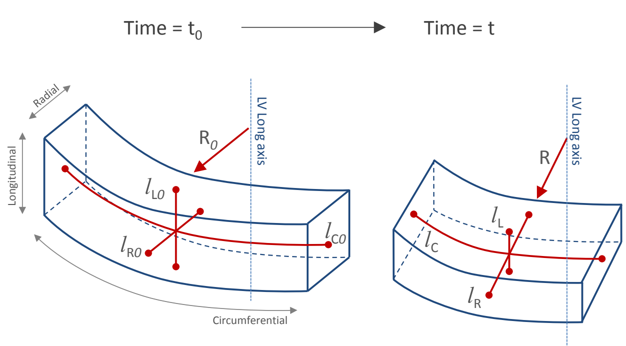


$$Rs = \frac{l_R - l_{R0}}{l_{R0}} \qquad Cs = \frac{l_C - l_{C0}}{l_{C0}}$$

$$Ls = \frac{l_L - l_{L0}}{l_{L0}} \qquad RS = \frac{R - R_0}{R_0}$$

Figure 2. Schematic of radial ($R_S$), longitudinal ($L_S$) and circumferential ($C_S$) strain and radial shortening (RS) computation in a portion of LV myocardium.

The software provides dynamic 3D connected meshes (862 vertices, 1720 triangular elements) of the LV endocardium and the value of the 3 components of strain for each node. The 3D meshes are then exported as ASCII files and imported into Matlab (Mathworks Inc). For each node, radial shortening (RS) was computed as the ratio of current distance from the node to the LV long axis (defined as the line joining the LV apex and the mid-point of the mitral valve) to the end-diastolic radius (Figure 2).

CTCA images were then exported in the DICOM format into Matlab to obtain the coronary tree geometry using custom software. First the images were filtered using a 3D non-linear median filter, and then the Frangi vesselness filter [6] was used to enhance the presence of vessel-like structures in the 3D dataset. Briefly, the Frangi vesselness $V$ filter is a multiscale filter that uses the eigenvalues $\lambda_i$ of the Hessian matrix to compute the likelihood of an image region to contain vessels, based on a weighted functional of 3 different measures (deviation from blob-like structure $R_B$, difference between plate-like and line-like structures $R_A$ and background noise $S$). For a given scale $\sigma$, the value of $V$ for the voxel $x$ is given by:

$$|\lambda_1| < |\lambda_2| < |\lambda_3|$$

$$\begin{cases} R_A = |\lambda_2| / |\lambda_3| \\ R_B = \sqrt{|\lambda_1| / |\lambda_2 \cdot \lambda_3|} \\ S = \sqrt{\sum_i \lambda_i^2} \end{cases}$$

$$V(\sigma, x) = \begin{cases} 0 & , \quad \lambda_2, \lambda_3 > 0 \\ 1 - e^{\frac{-R_A^2}{2\alpha^2}} \cdot e^{\frac{-R_B^2}{2\beta^2}} \cdot \left(1 - e^{\frac{-S^2}{2c^2}}\right) & , \text{otherwise} \end{cases}$$

The parameters α, β and c were set to be 0.5, 0.5 and 300 respectively [7]. The scale range σ was set to 3 voxels. The enhanced dataset was then used to extract the coronary artery tree in a two-step recursive algorithm with manual user interaction: first the centerline of the portion of the vessel included between two manually identified points was extracted as the shortest path resulting from the Dijkstra's algorithm using (1-voxel value) as edge cost [7]; second, a region growing algorithm was applied using the points belonging to the centerline as starting seeds.

Finally, the registration between the coronary tree and the 3D LV surface was performed using a landmark-based registration minimizing the least square distance between 3 pairs of landmarks specified by the user (aortic root, midpoint of the mitral valve and LV apex). The transformation matrix was calculated between the coronary tree and a mid-diastolic LV surface and then applied to all the dynamic surfaces.

# 3. Results

Three patients (12%) were excluded because of suboptimal quality of the CT images. Figure 3 shows the coronary tree with the LV surfaces color-coded for radial shortening in a normal subject at 3 different phases of the cardiac cycle. The composite display of coronary arteries and parametric images depicting wall motion allowed

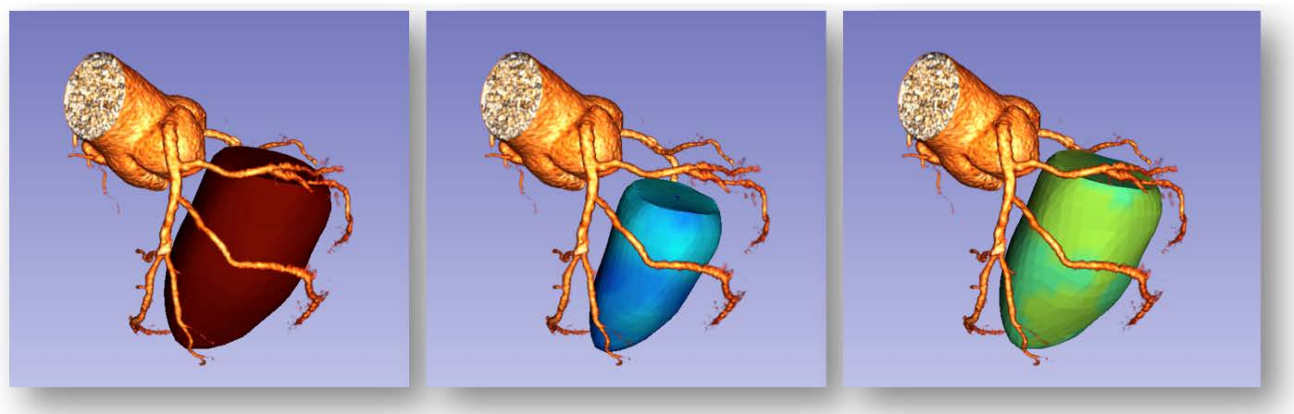

Figure 3. Pattern of LV radial shortening in a normal subject at 3 different phases of the cardiac cycle. From left to right: early systole (reference time point, RS=0%), end-systole (peak RS, with absolute RS values decreasing from apex to base) and mid-diastole (RS recovering).

visual appreciation of the functional significance of the coronary stenosis, when present. Patients with normal coronary arteries (N=18/21) had uniform parametric images of LV function (Figure 4).

In contrast, patients with significant stenosis had abnormal wall motion in the area supplied by the stenosed artery (Figure 5).

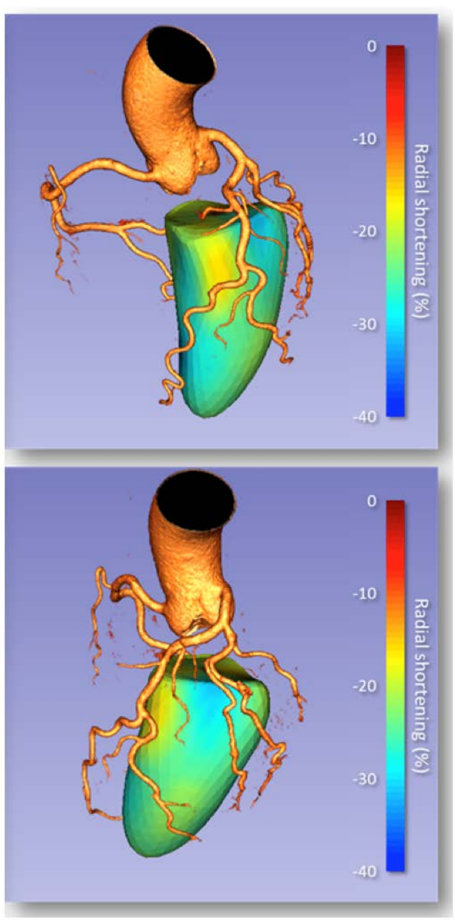


Figure 4. Distribution of radial shortening in a subject with normal coronary artery. In the absence of stenosis, the pattern of RS is uniform.

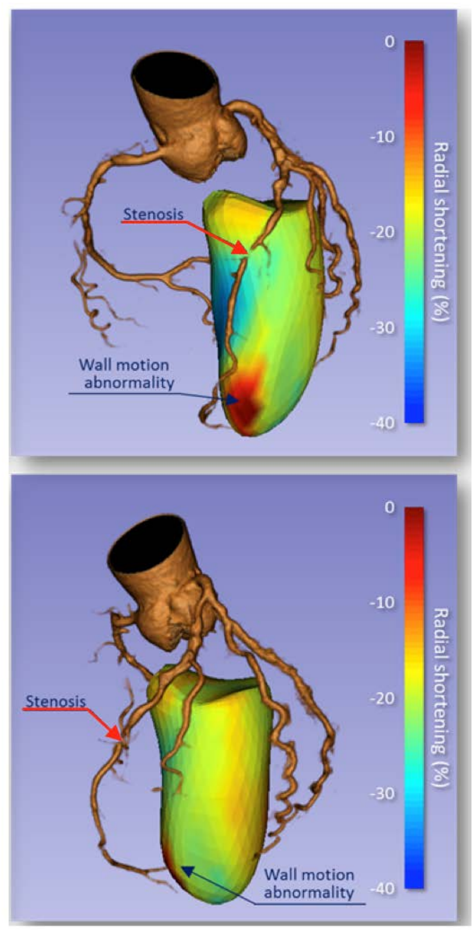


Figure 5. The near-complete occlusion in the mid left anterior descending artery (red arrows) was associated with reduced RS in the apical antero-septal region (blue arrows), supplied by this artery.

Interestingly, in a patient with biopsy-proven cardiac amyloidosis, both longitudinal and radial strain components showed a pattern of “apical sparing” (Figure 6), consistent with recent reports of lack of amyloid depositions near the apex observed on delayed-enhancement cardiac MRI [8].

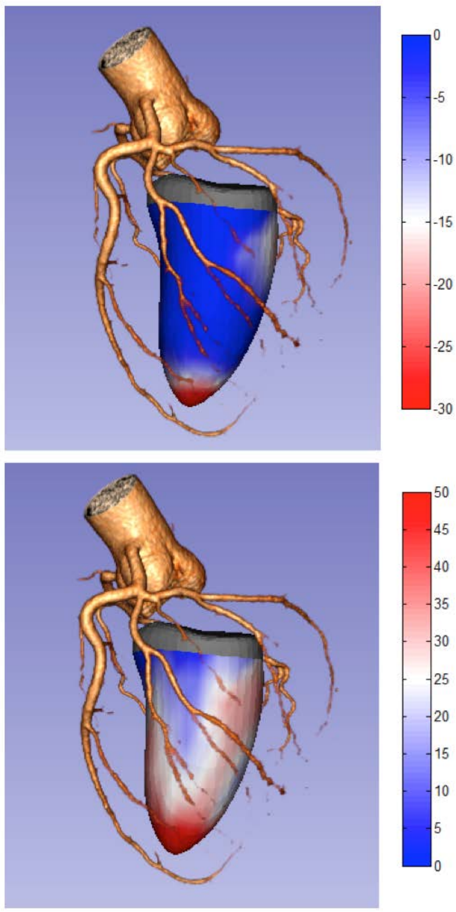


Figure 6. Example of longitudinal and radial strain distribution in a patient with cardiac amyloidosis and absence of any relevant coronary stenosis.

## 4. Conclusions

The results of this study indicate that fusion of CTCA and parametric imaging derived from 3DE is feasible, and may provide potentially physiologically meaningful and easy-to-interpret combined displays of coronary abnormalities and their functional impact. This approach is versatile, as it may be applied to a variety of parameters of cardiac mechanics. Importantly, it does not utilize additional ionizing radiation compared to the standard clinical protocol for the evaluation of coronary stenosis using CTCA, and is thus advantageous in terms of reduced risks to patients, as well as simplicity and cost savings.

## References

[1] Schroeder S, Achenbach S, Bengel F, Burgstahler C, Cademartiri F, de Feyter P, George R, Kaufmann P, Kopp AF, Knuuti J, Ropers D, Schuijf J, Tops LF, Bax JJ. Cardiac computed tomography: indications, applications, limitations, and training requirements: report of a Writing Group deployed by the Working Group Nuclear Cardiology and Cardiac CT of the European Society of Cardiology and the European Council of Nuclear Cardiology. Eur Heart J 2008;29:531-556.
[2] de Roos A. Myocardial perfusion imaging with multidetector CT: beyond lumenography. Radiology 2010;254:321-323.
[3] Deetjen AG, Conradi G, Mollmann S, Ekinci O, Weber M, Nef H, Mollmann H, Hamm CW, Dill T. Diagnostic value of the 16-detector row multislice spiral computed tomography for the detection of coronary artery stenosis in comparison to invasive coronary angiography. Clin Cardiol 2007;30:118-123.
[4] Geyer H, Caracciolo G, Abe H, Wilansky S, Carerj S, Gentile F, Nesser HJ, Khandheria B, Narula J, Sengupta PP. Assessment of myocardial mechanics using speckle tracking echocardiography: fundamentals and clinical applications. J Am Soc Echocardiogr 2010;23:351-369.
[5] Maffessanti F, Nesser HJ, Weinert L, Steringer-Mascherbauer R, Niel J, Gorissen W, Sugeng L, Lang RM, Mor-Avi V. Quantitative evaluation of regional left ventricular function using three-dimensional speckle tracking echocardiography in patients with and without heart disease. Am J Cardiol 2009;104:1755-1762.
[6] Frangi AF, Niessen WJ, Vincken KL, ViergeverMA Multiscale vessel enhancement filtering. In: Proceedings of medical image comput assisted intervention (MICCAI). Lecture notes in computer science 1998;1496:130–137.
[7] Yang G, Kitslaar P, Frenay M, Broerson A, Boogers MJ, Bax JJ, Reiber JHC, Dijkstra J. Automatic centerline extraction of coronary arteries in coronary computed tomographic angiography. Int J Cardiovasc Imaging 2012;28:921–933.
[8] Phelan D, Collier P, Thavendiranathan P, Popovic ZB, Hanna M, Plana JC, Marwick TH, Thomas JD. Relative apical sparing of longitudinal strain using two-dimensional speckle-tracking echocardiography is both sensitive and specific for the diagnosis of cardiac amyloidosis. Heart 2012;98:1442-1448.

Address for correspondence:

Francesco Maffessanti, PhD
University of Chicago Medical Center, M.C. 5084
5841 S Maryland Ave., 60637 Chicago, IL, USA
fmaffe@gmail.com